Journal of Inorganic and General Chemistry
ZAAC
Zeitschrift für anorganische und allgemeine Chemie
www.zaac.wiley-vch.de
RESEARCH ARTICLE
Check for updates
DOI: 10.1002/zaac.202300112

Special Collection

Synthesis and characterization of ternary trielides Na_7KTr_4 [*Tr* = In or Tl] including $[Tr_4]^{8-}$ Tetrahedra

Melissa Janesch,[a] Vanessa F. Schwinghammer,[a] Ilya G. Shenderovich,[b] and Stefanie Gärtner*[a, b]

In recognition of the outstanding scientific achievements by Prof. Dr. Eduard Zintl on the occasion of his 125th birthday

Two new ternary trielides Na_7KTr_4 (*Tr* = In, Tl) have been prepared by classical solid-state reaction from the elements in tantalum ampoules. Both are isostructural to Na_7RbTl_4 and therefore crystallize in the orthorhombic space group *Pbam*, Pearson symbol *oP*96 ($a = b = 16.3283(2)/16.2860(6)$, $c = 11.3094(17)/11.2771(4)$, $V = 3015.25(8)/2991.07(18)$, $Z = 8$, R_1, $wR_2 = 0.0249$, 0.0386/0.0447, 0.0608). The trielide subunit is built by two crystallographically independent $[Tr_4]^{8-}$ tetrahedra. ^{23}Na-MAS-Nuclear Magnetic Resonance (NMR) as well as EPR spectroscopy was employed to characterize the compounds further. DOS calculations showed a (pseudo) band gap at E_F for both compounds. Dissolution experiments in liquid ammonia were carried out for the two alkali metal indides Na_7KIn_4 and Na_2In according to the chemistry of group 14 and 15 *Zintl* anions. After evaporating the solvent, the remaining material was analyzed by powder X-ray diffraction and proved the formation of NaIn and $NaNH_2$.

Introduction

Since the discovery of NaTl in 1932 by *Eduard Zintl* himself,[1] alkali metal *Zintl* phases are still matter of current research as they provide the opportunity of discovering new (semi−)metallic materials of main group elements.[2–9] *Zintl* phases are electronically classified as intermetallic phases, assuming that an electron transfer from the less electronegative to the more electronegative elements takes place.[10,11] Hence, most of them are described as valence compounds and exhibit ionic as well as covalent bonding.[12,13] Concerning the combination of alkali metals and group 14 and 15 elements, a variety of isolated clusters can be found,[14,15] which can be described using the (8-*N*) rule.[16–18] According to the pseudo element concept,[19] tetrahedral $[Tt_4]^{4-}$ clusters are reported in binary materials $A_{12}Tt_{17}$ and A_4Tt_4 (*A* = Na–Cs, *Tt* = Si–Pb).[20–32] The combination of different alkali metals allowed for the observation of new structure types, e.g. $Rb_7Na(Ge_4)_2$,[32] $Cs_2Na_2Ge_4$[27] and $Li_{18}Na_2Ge_{17}$.[33] While these materials show that ordering can be observed, the solid solution of $K_{4-x}Na_xSi_4$ proves that mixed alkali metal sites are also possible.[23]

While the elements right to the *Zintl* border have been intensely studied concerning their structural chemistry, alkali metal trielides still provide a large scope of research.[34,35] Initially, they were not considered as very promising candidates to build deltahedral clusters like group 14 and 15 elements do as they are located left to the *Zintl* border in the periodic table.[10] However, further investigations revealed a vast variety of different clusters with delocalized bonding.[36] Due to its inert 6s electron pair thallium exhibits a large and diverse richness of isolated clusters.[37] Typically, these naked thallium clusters exhibit high negative charges as is observed e.g. for $[Tl_4]^{8-}$, $[Tl_5]^{7-}$, $[Tl_6]^{6-}$, $[Tl_6]^{8-}$, $[Tl_7]^{7-}$ $[Tl_9]^{9-}$ or $[Tl_{11}]^{7-}$.[38–45] The lighter homologue gallium, in contrast, forms intercluster bondings to compensate these high charges.[46–49] Indium is located at the borderline between thallium and the lighter group 13 elements.[50–58] Investigations on the incorporation of different, closed shell complex anions into the alkali metal - triel system allowed for the observation of isolated hypoelectronic $[Tr_6]^{6-}$ or $[Tr_{11}]^{7-}$ indium and also thallium clusters.[59–62] Besides that, isolated indium $[In_5]$ clusters are reported in $(Ba_6N)[In_5]$[63] and in the more complex $(Ba_{38}N_{18})[In_5]_2[In_8]$,[64] where next to the $[In_5]$ clusters also $[In_8]$ clusters are present. Further, tetrahedral $[In_4]$ subunits are observed in Tm_4IrIn_4, Lu_4PtIn_4, Gd_5RhIn,[65–67] $(A_{19}N_7)[In_4]_2$ (*A* = Sr, Ca)[68] and Na_2In.[69] While tetrahedral clusters of thallium are present in different alkali metal thallides like $Na_{23}K_9Tl_{15.3}$[70] or Na_2Tl,[38] isostructural Na_2In is the exclusive representative including $[In_4]^{8-}$ within the alkali metal – indium system. Here, the *Zintl-Klemm* concept[13,71,72] works well, as the

[a] *M. Janesch, V. F. Schwinghammer, Dr. S. Gärtner*
Department of Inorganic Chemistry
University of Regensburg
93040 Regensburg
E-mail: Stefanie.Gaertner@ur.de
[b] *Dr. I. G. Shenderovich, Dr. S. Gärtner*
Central Analytics
University of Regensburg
93040 Regensburg

Supporting information for this article is available on the WWW under https://doi.org/10.1002/zaac.202300112

Special Collection *This article is part of a Special Collection to celebrate Professor Eduard Zintl on the occasion of his 125th anniversary. Please see our homepage for more articles in the collection.*

Table 1. Crystallographic data and structure refinement parameters for Na_7KTr_4 (Tr = In, Tl).

Empirical Formula	Na_7KIn_4	Na_7KTl_4
CSD number	2257763	2262417
Formula weight	659.31	1018.63
Temperature/K	123.00(10)	123.01(10)
Crystal System	orthorhombic	
Space group	*Pbam*	
$a = b$/Å	16.3283(2)	16.2860(6)
c/Å	11.3094(17)	11.2771(4)
Volume/Å^3	3015.25(8)	2991.07(18)
Z	8	
ρ_{calc}/(g/cm^3)	2.905	4.519
μ/mm^{-1}	3.4	23.5
F(000)	2336.0	3364.0
Crystal size/mm^3	0.118 × 0.078 × 0.056	0.047 × 0.022 × 0.011
Radiation λ/Å	AgKα (0.56087)	
2θ range for data collection/°	4.9 to 65.8	4.9 to 51.1
Index ranges	$-30 \le h \le 30$ $-31 \le k \le 31$ $-21 \le l \le 21$	$-25 \le h \le 25$ $-25 \le k \le 24$ $-17 \le l \le 17$
Collected/Independent Reflections	99831/11316	43625/5943
Data/restraints/parameters	11316/0/126	5943 / 0 / 126
Goodness-of-fit on F^2	1.054	1.191
R_{int}	0.0334	0.0543
Final R indexes [$I \ge 2\sigma(I)$]	$R_1 = 0.0191$, $wR_2 = 0.0363$	$R_1 = 0.0383$, $wR_2 = 0.0595$
Final R indexes [all data]	$R_1 = 0.0249$, $wR_2 = 0.0386$	$R_1 = 0.0447$, $wR_2 = 0.0608$
Largest diff. peak/hole/e Å^{-3}	2.24/−1.31	3.52/−2.70
Flack parameter	0.6142(4)	0.5355(8)

less electronegative sodium atom transfers its 3s electron to the more electronegative group 13 element, which formally results in $(Na^+)_2Tr^{2-}$ (Tr = In, Tl). Thus, the Tr^{2-} anion is isoelectronic to a group 15 element and forms tetrahedral $[Tr_4]^{8-}$ clusters, which are valence-isoelectronic to P_4 or As_4 units in white phosphorous and yellow arsenic[73] which is in accordance to the pseudo element concept.[19] In general, it has been shown for thallides, that the alkali metal employed plays a major role for the structural chemistry of the observed materials.[74] We now extended this concept for the lighter element indium.

Here we report on the preparation and characterization by single crystal X-ray structure analysis and ^{23}Na-NMR spectroscopy of Na_7KTr_4 (Tr = In, Tl). Na_7KIn_4 is the first ternary compound and only the second alkali metal indide beside Na_2In with isolated $[In_4]^{8-}$ tetrahedra. Additionally, preliminary dissolution studies in liquid ammonia were carried out for the alkali metal indides Na_7KIn_4 and Na_2In.

Results and Discussion

Preparation and structure description

The two ternary compounds Na_7KTr_4 (Tr = In, Tl) were characterized by single crystal X-ray structure analysis (Table 1) and are isostructural to Na_7RbTl_4[75] (see SI for the atomic coordinates and displacement parameters). Therefore, the structures were compared with the Bilbao Crystallographic Server (BCS) using the program COMPSTRU.[76–79] Table 2 gives the lattice and atomic position criteria of the evaluation of the structure similarity. The degree of lattice distortion (S) is the spontaneous strain, the maximum distance ($d_{max.}$) gives the maximal displacement between the atomic positions of the paired atoms and d_{av} is the arithmetic mean of the distance. The function of the differences in atomic positions (weighted by the multiplicities of the sites) and the ratios of the corresponding lattice parameters of the structure is the measure of similarity (Δ). The measure of similarity is 0.006 for Na_7KIn_4 or 0.003 for Na_7KTl_4 respectively (see Table 2) and proves that these two structures are highly similar to Na_7RbTl_4. Compared to other S- or Δ-values found in the literature[80–82] they are very small indicating a high similarity of these three ternary compounds, which is expected for compounds of the same structure type.

Concerning preparation of these materials, it turned out that the temperature program plays a crucial role for the outcoming product. While Na_7RbTl_4 and Na_7KIn_4 were cooled

Table 2. Lattice and atomic position criteria of the BCS evaluation of the structure similarity.

Compound	S	$d_{max.}$ (Å)	d_{av} (Å)	Δ
Na_7KIn_4	0.0012	0.0914	0.0558	0.006
Na_7KTl_4	0.0027	0.0795	0.0288	0.003

down slowly with 5 K/h to room temperature, Na_7KTl_4 was only obtained after quenching with water. A slow cooling rate resulted in a mixture of Na_2Tl, $Na_{14}K_6Tl_{18}$ and supposably Na_7KTl_4 in very small amounts (see SI). Refinement of the lattice obtained by the optimized experimental procedure resulted in Na_7KTl_4 (see SI). First DSC measurements of all three compounds show a first endothermic peak during heating, followed by a second endothermic peak at higher temperature (see SI). Upon cooling, several effects are observed. As nothing is known about the ternary Na-*A*-*Tr* phase diagram yet, no phase and/or transition can be unambiguously assigned to the additional peaks. These observations mean a clear demand on further detailed investigations. According to the structure type Na_7RbTl_4, Na_7KTr_4 is described in the orthorhombic space group *Pbam* and contains six crystallographically independent *Tr* positions (*Tr* = In, Tl) as well as 12 crystallographically independent alkali metal positions. The two symmetry inequivalent $[Tr_4]^{8-}$ tetrahedra are each built from three *Tr* atoms: *Tr*1, *Tr*5, *Tr*6 (tetrahedron 1) and *Tr*2, *Tr*3, *Tr*4 (tetrahedron 2). Every *Tr* tetrahedron is coordinated by 16 sodium atoms and five potassium atoms. In analogy to Na_7RbTl_4, Na_7KTr_4 also show pseudo-merohedral twinning.[75]

Distortion of the $[Tr_4]^{8-}$ tetrahedra

Comparing the crystal structures of Na_7KIn_4 and Na_7KTl_4, the $[In_4]^{8-}$ tetrahedra show less distortion from the ideal tetrahedron geometry (tetrahedron 1: 4.5°, tetrahedron 2: 2°) regarding the observed angels as well as the *Tr*-*Tr* distances. These distances are for Na_7KIn_4 in closer range (3.0227(2) Å to 3.1724(3) Å) than for the heavier homologue (3.1306(6) Å to 3.4606(9) Å), where each tetrahedron always exhibits one short and one long edge (see Table 3). Therefore, the In–In distances are shorter than the Tl–Tl lengths in Na_7RbTl_4 (3.1366(3) Å to 3.4408(4) Å)[75] but comparable to similar distances e.g. in Na_2In, where the intracluster distances range from 3.0617(2) Å to 3.1493(1) Å.[69] The reasons for the different values of the distortion might be due to packing effects and also being biased by the intrinsic pseudo-merohedral twinning, detailed theoretical investigations for a deeper understanding of the intracluster interactions are currently in progress.

Table 4 gives an overview of the interatomic *Tr*-*Tr* distances of the here reported and of the literature compounds which exhibit $[Tr_4]$ tetrahedra (*Tr* = In, Tl).

Table 4. *Tr*-*Tr* distances in binary and ternary compounds showing $[Tr_4]$ building units. For the $GdRhIn_4$ structure type not all compounds are listed here but they are known for *RE* = Gd–Er.

Compound	Space Group	d(*Tr*-*Tr*) [Å]	Reference
Na_2In	$C222_1$	3.0612(1)–3.1493(1)	[69]
Na_2Tl	$C222_1$	3.1676(3)–3.2863(3)	[38]
Na_7KIn_4	*Pbam*	3.0226(2)–3.2642(3)	reported here
Na_7KTl_4	*Pbam*	3.1309(6)–3.4609(9)	reported here
Na_7RbTl_4	*Pbam*	3.1366(3)–3.4408(4)	[75]
Tm_4IrIn	$F\bar{4}3m$	3.175	[67]
Lu_4PtIn	$F\bar{4}3m$	3.184	[67]
$GdRhIn_4$	$F\bar{4}3m$	3.171	[66]
$Gd_4IrInO_{0.25}$	$F\bar{4}3m$	3.182(1)	[65]
$(Ca_{19}N_7)[In_4]_2$	$Fm\bar{3}m$	3.116(3)	[68]
$(Sr_{19}N_7)[In_4]_2$	$Fm\bar{3}m$	3.097(3)	[68]
$Na_{23}K_9Tl_{15.3}$	$P6_3/mmc$	3.271(3)–3.281(2)	[70]

Alkali metal coordination

Since the two compounds Na_7KTr_4 (*Tr* = In, Tl) are isostructural to Na_7RbTl_4, they exhibit two symmetry inequivalent potassium atoms as well as ten symmetry inequivalent sodium atoms. While for potassium the number of neighbouring atoms calculates to a value of 18, for the sodium atoms 11, 12, or 14 neighbouring atoms are found.

The K–In distances in Na_7KIn_4 range from 3.8 to 4.1 Å and hence are in the range of observed distances in other ternary alkali metal indides, e.g. in $K_3Na_{26}In_{48}$ (*d*(K–In) = 3.5 to 4.2 Å)[58] or KNa_3In_9 (*d*(K–In) = 3.9 to 4.1 Å).[57] The Na–In distances range from 3.1 to 3.5 Å and are again comparable with the ternary alkali metal indides $K_3Na_{26}In_{48}$ or KNa_3In_9, in which the Na–In distances range from 3.2 to 3.7 Å respectively from 3.2 to 3.7 Å.[57,58] The same is true for the Na–K distances, which are between 3.6 and 4.4 Å. In $K_3Na_{26}In_{48}$ *d*(Na–K) are around 3.8 Å[58] and in KNa_3In_9 *d*(Na–K) are about 4.0 Å.[57] K–Tl distances in the heavier homologue Na_7KTl_4 range from 3.7 to 4.0 Å and therefore they are comparable with K–Tl distances in the ternary compounds $Na_{23}K_9Tl_{15.3}$ (*d*(K–Tl) = 3.9 to 4.7 Å)[70] or $Na_9K_{16}Tl_{25.25}$ (*d*(K–Tl) = 3.7 to 4.3 Å).[83] The same can be observed for the Na–Tl distances which are between 3.1 to 3.5 Å. Again, they are in the range of distances in the ternary alkali metal thallides $Na_{23}K_9Tl_{15.3}$ (*d*(Na–Tl) = 3.2 to 3.5 Å)[70] or $Na_9K_{16}Tl_{25.25}$ (*d*(Na–Tl) = 3.3 to 3.3 Å).[83] Na–K distances in Na_7KTl_4 reach from 3.7 to 4.2 Å and are again similar to the ternary compounds $Na_{23}K_9Tl_{15.3}$ (*d*(Na–Tl) = 3.9 to 4.1 Å)[70] or $Na_9K_{16}Tl_{25.25}$ (*d*(Na–Tl) = 3.7 to 4.0 Å).[83]

Table 3. Distortion of the two crystallographically inequivalent Tetrahedra 1 and 2 in Na_7KTr_4 (*Tr* = In, Tl).

	Tetrahedron	Max. deviation of ideal 60° angle	d(*Tr*-*Tr*) [Å]
Na_7KIn_4	**1** (In1, In5, In6)	4.5°	3.0227(2)–3.1691(3)
	2 (In2, In3, In4)	2.0°	3.0319(2)–3.1724(3)
Na_7KTl_4	**1** (Tl1, Tl5, Tl6)	6.2°	3.1306(6)–3.4606(9)
	2 (Tl2, Tl3, Tl4)	3.1°	3.1406(6)–3.2881(8)

The structure description of the structure type Na_7RbTl_4 focused on the large entities within the unit cell (Rb^+ cations and $[Tl_4]^{8-}$ anions). There, a distorted cubic closest packing of the tetrahedra was reported.[75] The rubidium atoms reside in the octahedral voids of this packing. This of course still is true for the isostructural compounds Na_7KTr_4 we report on in the present case. Additionally, we want to elucidate the role of the sodium atoms within the three-dimensional arrangement. In the close-packed case, it is useful to subdivide the network according to the present symmetry and consecutively, four different alkali metal subunits can be described. Their centers are located on Wyckoff position 2*a* (structural subunit A), 2*b* (structural subunit B), 2*c* (structural subunit C) and 2*d* (structural subunit D) (see Figure 1). They are all interconnected either by the $[Tr_4]^{8-}$ tetrahedra or by Na6 and Na8 atoms. In the crystallographic *c*-direction they interpenetrate (see Figure 2).

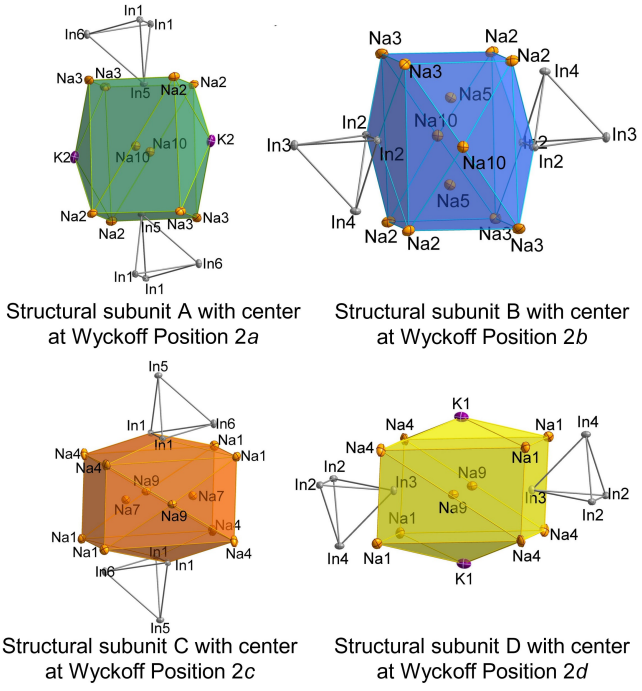

Figure 1. The four different structural subunits built by the alkali metals with their centers at the corresponding Wyckoff positions.

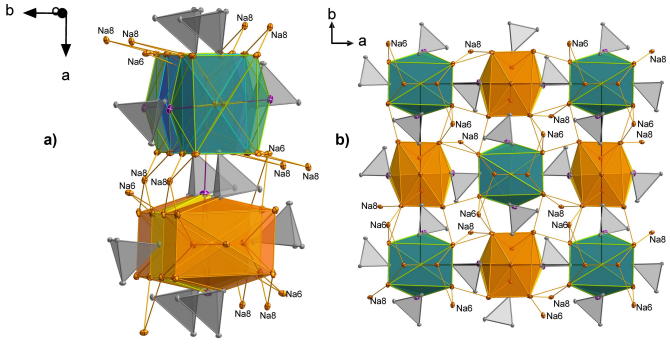

Figure 2. a) Structural subunit A (green) and C (orange) are interconnected in *a*-direction by tetrahedron 1 and Na8, which coordinates via one vertex to structural subunit A and via one edge to structural subunit C. The same can be observed for the structural subunits B and D. They are interconnected in *b*-direction by tetrahedron 2 and Na6, which coordinates via one vertex to structural subunit D and via one edge to structural subunit B. b) Packing of the four structural subunits in the unit cell.

All four structural subunits are built by two symmetry inequivalent sodium atoms, which form a distorted cuboid. The two opposite rectangular faces are capped by a sodium atom (Na9 or Na10) or potassium atom (K1 or K2). Na2 and Na3 form the cuboid with the center on Wyckoff position 2*a* and K2 caps two opposite faces. To the remaining pair of rectangular faces is coordinated by one vertex of $[Tr_4]^{8-}$ tetrahedron 1. The cuboid with the center on Wyckoff position 2*b* is also built by Na2 and Na3. Here, tetrahedron 2 coordinates via one edge to the one pair of opposite faces and the other two faces are capped by Na10 atoms. Hence the alkali metal subunits A and B are interpenetrating in the crystallographic *c*-direction since the two Na10 atoms are located inside polyhedron A.

In the remaining structural subunits with the center on Wyckoff position 2*c* and 2*d*, the cuboid body is formed by Na1 and Na4. In structural subunit C, the two rectangular faces are capped by Na9 and tetrahedron 1 coordinates with an edge. In structural subunit D, K1 caps the faces and tetrahedron 2 is coordinated via one vertex to the other pair of faces. These two structural subunits also interpenetrate in the crystallographic *c*-direction because Na9 caps the rectangular faces of structural subunit C and at the same time it is located in the cavity of structural subunit D.

Structural subunit A and C are interconnected in the crystallographic *a*-direction by tetrahedron 1 as well as by Na8. Tetrahedron 2 and the Na6 atom connects structural subunit B with structural subunit D in the crystallographic *b*-direction (see Figure 2 a)). Altogether, a dense network of the polyhedral subunits described above is observed in the unit cell of Na_7ATr_4, in which the $[Tr_4]^{8-}$ tetrahedra are embedded. This regular arrangement of sodium atoms is in strong contrast to the one observed for Na_2Tr. In this binary case, a more irregular sodium network is present (see SI, Figure 1).

Magnetic resonance studies: ^{23}Na-NMR and EPR Spectroscopy

In order to retrieve information about the para – or diamagnetic situation of Na_7ATr_4 and Na_2Tr materials, EPR measurements were carried out (see SI, Figure 2). As no signal was detected, further investigations using NMR were possible. Figure 3 shows the static ^{23}Na-NMR spectrum of Na_7KIn_4. This spectrum is a superposition of signals from ten crystallographically distinct sites: four sodium atoms at the Wyckoff position 8*i* (Na1-Na4), two sodium atoms at the positions 4*h* (Na5, Na6) and 4*g* (Na7, Na8) each, and one sodium atom at the positions 4*f* (Na9) and 4*e* (Na10) each (see Figure 3). The definite determination of the spectroscopic parameters of these sites is not possible as overlapping signals are expected due to similar but not identical surroundings of the respective sites. It is only possible

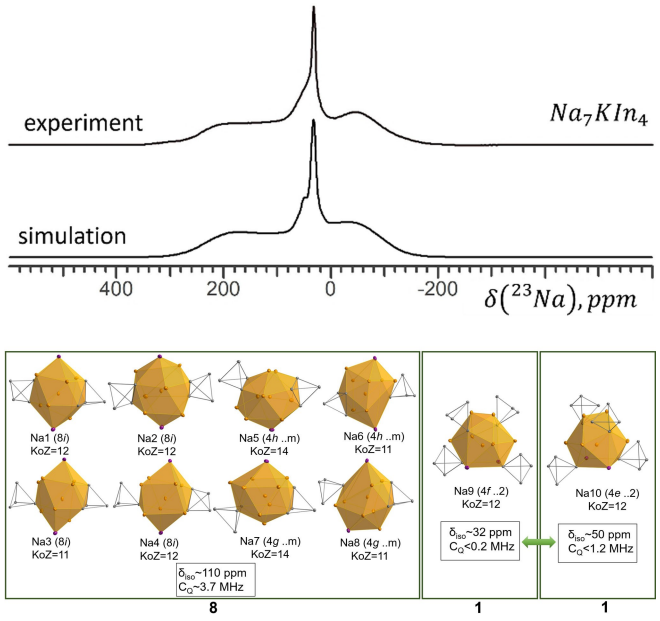

Figure 3. The experimental and simulated ^{23}Na NMR spectra of Na_7KIn_4. In the upper picture the experimental as well as the simulated signal is depicted. Below, the coordination spheres around the ten crystallographically different sodium atoms are illustrated. Na1–Na8 show a more asymmetric environment and are responsible for the broad signal at δ_{iso} ~110 ppm. Na9 and Na10 exhibit a more symmetric coordination sphere and therefore are responsible for the two sharp signals at δ_{iso}~50 ppm and at δ_{iso}~32 ppm respectively.

to roughly decompose this experimentally detected signal into three components with relative intensities of 8:1:1. The estimated spectroscopic parameters of the main signal are $\delta_{iso} \approx 110$ ppm, $C_Q \approx 3.7$ MHz, $\eta \approx 0$, of the second signal: $\delta_{iso} \approx 50$ ppm, $C_Q \approx 1.2$ MHz, $\eta \approx 1$, and of the third signal: $\delta_{iso} \approx 32$ ppm, $C_Q < 0.2$ MHz. The simulation of the decomposed experimentally detected signal is shown in Figure 3. The first signal at 110 ppm can be tentatively assigned to the eight sodium atoms on Wyckoff sites 8*i*, 4*h*, and 4*g*. The sharp signals from Na9 and Na10 can be attributed to the positions 4*f* and 4*e* or vice versa. The small linewidth of these signals is a result of the symmetric surrounding of these alkali metal positions. Na9 and Na10 are almost tetrahedrally surrounded by four $[In_4]^{8-}$ clusters. The remaining eight sodium positions exhibit a more asymmetric coordination sphere including only two $[In_4]^{8-}$ subunits.

The ^{23}Na NMR spectrum of Na_7KIn_4 deviates strongly from the ^{23}Na NMR spectra of Na_7RbTl_4, Na_2Tl, and Na_2In (see SI, Figure 3). The latter do not have narrow components and their intensity maxima are at 250 ppm, 300 ppm, and 150 ppm, respectively. It is assumed, that the broad signal in Na_2In can be derived from the more asymmetric packing of the sodium atoms.

Calculation of the electronic structure

Theoretical calculations revealed a (pseudo) band gap for Na_7KTr_4 around the Fermi level, which is typical for *Zintl* phases (see SI Figure 4–7).[84,85] As Na_7KIn_4 is built from $[In_4]^{8-}$ tetrahedra, which follow the (8-*N*) rule,[86] each edge of the tetrahedra corresponds to an electron precise two-center-two-electron bond. This is according to the *Zintl-Klemm* concept, where a complete electron transfer from the less electronegative alkali metals to the more electronegative indium is supposed.[13,71,72] This in return leads to a closed shell configuration on the triel.[10] This is reflected in the total DOS of the compound (see SI).

Dissolution experiments in liquid ammonia

Liquid ammonia is well suited for dissolving high negatively charged homoatomic polyanions.[17,18,71]

Most of the *Zintl* anions of group 14 elements can be dissolved in liquid ammonia.[32] This is also true for most of the $[Tt_4]^{4-}$ tetrahedra in combination with the alkali metals.[24,87,88] For trielid $[Tr_4]^{8-}$ tetrahedra no such dissolution has been observed so far. We recently reported on a blue solution for Na_2Tl and Na_7RbTl_4, what is a sign for solvated electrons.[75] The residue after evaporation of liquid ammonia was elemental thallium and sodium amide. This indicated a fast decomposition of the compounds upon dissolution. Therefore, it is supposed that the $[Tl_4]^{8-}$ tetrahedra and trielid clusters in general exhibit a too high negative charge per atom to be transferred into solution. To the best of our knowledge, the naked cluster anion $[Bi_4]^{6-}$ with a negative charge of −1.5 per atom is the highest negatively charged entity, which can be transferred into solution yet.[89]

As the In–In bond strength is assumed to be stronger than Tl–Tl bonds[90,91] dissolution experiments in liquid ammonia were examined for the two alkali metal indides Na_7KIn_4 and Na_2In. For the first one a blue solution was observed, which turned into a clear and colorless solution after one month of

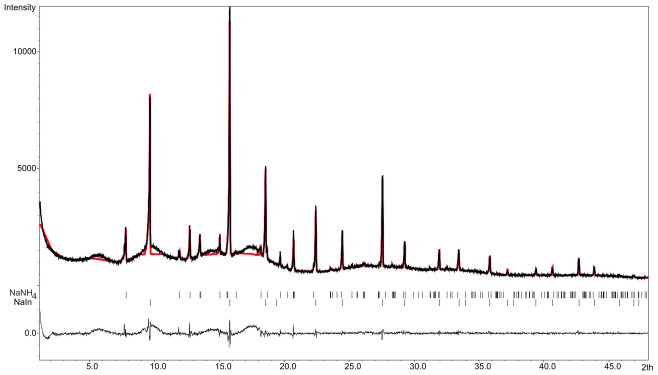

Figure 4. Powder diffraction pattern of the product of Na_7KIn_4 after evaporation the liquid ammonia. $NaNH_2$ and NaIn were refined using the LeBail algorithm with GOF = 2.15, R_p = 5.08, wRp = 6.91.

storage at 233 K and a black residue could be observed. The binary Na_2In, however, showed a clear and colorless solution.

After one month of storage at 233 K, a yellow-greenish solution with black residue was observed. After evaporation of the liquid ammonia, the residue of both compounds was characterized by X-ray powder diffraction experiments. For Na_7KIn_4, alkali metal amide as well as NaIn were obtained (see Figure 4), whereas for Na_2In alkali metal amide, NaIn as well as elemental indium were identified as products (see SI). These preliminary experiments show that a stepwise oxidation of the $[In_4]^{8-}$ tetrahedra occurs in liquid ammonia solution. Detailed solution studies are currently in progress in order to investigate the reactivity of the $[In_4]^{8-}$ tetrahedra in liquid ammonia.

Conclusions

We here report on the synthesis and characterization of the two ternary compounds Na_7KTr_4 (Tr = In, Tl), which are isostructural to Na_7RbTl_4. These compounds were prepared by classical high temperature solid state synthesis. Thereby it turned out, that the temperature program plays a crucial role for the outcoming product. Whereas Na_7RbTl_4 and Na_7KIn_4 were obtained after slow cooling, the synthetic route for Na_7KTl_4 is a different one since it was quenched with water to room temperature. Theoretical calculations using *FPLO21* revealed a (pseudo) band gap at E_F for the two ternary compounds Na_7KTr_4 (Tr = In, Tl), what indicates a semi-metallic character. Na_7KIn_4 is the first ternary alkali metal indide with isolated $[In_4]^{8-}$ tetrahedra. Therefore, solvation tests in liquid ammonia were carried out for this compound and the binary Na_2In, which is built from the same type of naked indium clusters. In contrast to the thallides, which compose rapidly to elemental thallium and alkali metal amide, the indides Na_2In and Na_7KIn_4 form binary NaIn and alkali metal amide upon dissolution in liquid ammonia. The oxidation of a small $[In_4]^{8-}$ *Zintl* anion precasted in solid state in the compounds Na_2In or Na_7KIn_4 in liquid ammonia solution can be interpreted as first evidence for a reactivity of trielides according to the well-established chemistry of salt-like tetrelides in this solvent.[92–95] Future experiments will show, if the isolation of intermediates support this idea.

Experimental Section

Materials: Sodium and potassium (purity 99%, under mineral oil, Merck/Sigma-Aldrich, Darmstadt) were segregated for purification. Indium drops (purity 99.99%, ABCR) and thallium drops (purity 99.999% ABCR) were used without further purification and were stored under an inert gas atmosphere. Due to the high toxicity of the element thallium we have a separate fume cupboard, where all instruments, which were used for the work with thallium are placed. Outside the glovebox all these instruments as well as the tantalum ampoules are only touched with gloves.

Preparation: Due to the fact that the alkali metal indides and thallides are very sensitive towards air and moisture, all operations are performed under inert gas atmosphere in a glove box (Labmaster 130 G, Fa. M. Braun, Garching, Germany). For the synthesis of Na_7KTr_4 (Tr = In, Tl) the elements were placed in a tantalum ampoule, which was sealed in argon atmosphere. The sealed ampoules were placed in quartz glass tubes (QSIL GmbH, Ilmenau, Germany) and sealed again under argon atmosphere. The following temperature program was used: heating from room temperature to 773.15 K with a heating rate of 100 K/h, holding for 48 h then cooled with a cooling rate of 100 K/h to 473.15 K, which were held for 48 h. After that it was cooled to room temperature with a cooling rate of 5 K/h. In case of Na_7KTl_4 the ampoule was quenched to room temperature after holding for 48 h.

Solvation experiments in liquid ammonia: In the glove box the compounds were weighted into a *Schlenk* flask, which was baked out three times before. After that, liquid ammonia was condensed at 195 K on the products using *Schlenk* technique. For evaporation also *Schlenk* technique was used again at 195 K. The residue was taken out in the glove box and pestled in a mortar.

DSC measurements: The compounds Na_7ATr_4 (A = K, Rb and Tr = In, Tl) were filled into an aluminium crucible, which was subsequently clamped shut. The sample was heated in a continuous nitrogen flow, from 298 K to 573 K and cooled back to 298 K with a heating and cooling rate of 10 K min^{-1}. All measurements were performed on a METTLER TOLEDO DSC (METTLER TOLEDOO Gießen, Germany). With a DSC30 measuring cell, with the software METTLER TOLEDO STAR^e 5.1 used for evaluation purposes.

X-Ray Single Crystal Analysis: A small number of crystals was transferred into vacuum dried mineral oil. A suitable crystal was selected and mounted on a Rigaku SuperNova diffractometer (Rigaku Polska sp. Z. o. o. UI, Wroclaw, Poland) (X-ray: Ag microfocus, AtlasS2 detector) using MiTeGen loops. All data were collected at 123 K.

For data collection and data reduction *CrysAlisPro* (Version 41_64.93a)[96] was used. The structure solution was carried out with *ShelXT*[97] and for the subsequent data refinement *ShelXL*[98] was applied. For visualization purposes *Olex*^{2} was used and the software *Diamond4* was chosen for the representation of the crystal structure. All atoms are depicted as ellipsoids with a 50% probability level.

Crystallographic data for the compounds have been deposited in the Cambridge Crystallographic Data Center, CCDC, 12 Union Road Cambridge CB21EZ, UK. Copies of the data can be obtained free of charge under the depository number CCDC-2257763 or CCDC-2262417 http://www.ccdc.cam.ac.uk).

Powder Diffraction Studies: Powder diffraction samples were prepared in sealed capillaries (∅ 0.3 mm, WJM-Glas-Müller GmbH, Berlin, Germany). The data collection was carried out on a STOE Stadi P diffractometer (STOE, Darmstadt, Germany) (Monochromatic MoKα1 radiation, λ = 0.70926 Å for Na_7KTl_4 and Na_2In monochromatic CuK α1 radiation, λ = 1.54056 Å for the ternary alkali metal indide) equipped with a Dectris Mythen 1 K detector. For the refinement with the leBail algorithm the software JANA2006 was used.[99]

Magnetic resonance measurements: NMR measurements were performed on an Infinity$_{plus}$ spectrometer system (Agilent) operated at 7 T, equipped with a Chemagnetics–Varian 6 mm pencil cross polarization magic angle spinning (CPMAS) probe. Spectra were recorded using a 90°pulse of 5.0µs and a relaxation delay of 1 s. The spectra were indirectly referenced to NaCl (1 M in H_2O). The X band EPR measurements were carried out with a MiniScope MS400 device with a frequency of 9.5 GHz and rectangular resonator TE102 of the company Magnettech GmbH. The experimental NMR spectrum of Na_7KIn_4 was modeled using the WSolids1 software package.[100]

DFT Calculations: The program FPLO21[101–104] was used for the theoretical calculations, which is based on the full-potential non-orthogonal local orbital minimum-basis within the generalized gradient approximation (GGA) for full-relativistic mode. Therefore, a full-relativistic approach is necessary because a neglection of the spin-orbit coupling (SOC) leads to different results than using the full-relativistic approach.[105] The exchange correlation was assumed in the form proposed by Perdew, Burke and Ernzerhof (PBE).[106] For the calculation of the density of states (DOS) two modular grids for the reciprocal space were tried out one with 216 k-points and the other one with 1000 k-points. It turned out, that 216 k-points are sufficient. A change of the total energy ($\Delta E_{tot} \leq 10^{-6}$ Hartree) was used as convergence criterion. For the visualisation of the band structure the program xfbp[96–99] was used and the DOS was plotted with Origin2020 (version 9.7.0.188).[107]

Acknowledgements

The authors thank Prof. Pfitzner for providing lab equipment and Prof. N. Korber for providing lab equipment as well as for very valuable discussions. The authors are indebted to Dr. G. Balázs for recording the EPR spectra, Franziska Kamm (AK Prof. Pfitzner) for the powder diffraction experiments and Ulrike Schießl (AK Prof. Pfitzner) for the DSC measurements. This research was founded by the Frauenförderung of the University of Regensburg and the German Science Foundation (DFG) (GA 2504/1-1). Open Access funding enabled and organized by Projekt DEAL.

Conflict of Interest

The authors declare no conflict of interest.

Data Availability Statement

The data that support the findings of this study are available in the supplementary material of this article.

Keywords: Indium · Thallium · solid state ^{23}Na NMR · Single Crystal · Liquid Ammonia

[1] E. Zintl, W. Dullenkopf, *Z. Phys. Chem.* **1932**, *16B*, 195–205.
[2] T. F. Fässler, S. Hoffmann, *Z. Anorg. Allg. Chem.* **2000**, *626*, 106–112.
[3] L. Deakin, R. Lam, F. Marsiglio, A. Mar, *J. Alloys Compd.* **2002**, *388*, 69–72.
[4] F. Gascoin, S. Ottensmann, D. Stark, S. M. Haïle, G. J. Snyder, *Adv. Funct. Mater.* **2005**, *15*, 1860–1864.
[5] J. Jiang, A. C. Payne, M. M. Olmstead, H. O. Lee, P. Klavins, Z. Fisk, S. M. Kauzlarich, R. P. Hermann, F. Grandjean, G. J. Long, *Inorg. Chem.* **2005**, *44*, 2189–2197.
[6] J. Jiang, S. M. Kauzlarich, *Chem. Mater.* **2006**, *59*, 435–441.
[7] S. M. Kauzlarich, S. R. Brown, G. Jeffrey Snyder, *J. Chem. Soc. Dalton Trans.* **2007**, 2099–2107.
[8] M. Beekman, S. M. Kauzlarich, L. Doherty, G. S. Nolas, *Materials* **2019**, DOI 10.3390/ma12071139.
[9] C. Chen, W. Xue, S. Li, Z. Zhang, X. Li, X. Wang, Y. Liu, J. Sui, X. Liu, F. Cao, Z. Ren, C. W. Chu, Y. Wang, Q. Zhang, *Proc. Nat. Acad. Sci.* **2019**, *116*, 2831–2836.
[10] A. M. Guloy, in *Inorganic Chemistry in Focus III*, WILEY-VCH Verlag GmbH & Co.KGaA, Weinheim, **2006**, pp. 157–171.
[11] S. C. Sevov, in *Intermetallic Compounds - Principles and Practice* (Ed.: J. H. Westbrook, R. L. Fleischer), **2002**, pp. 113–132.
[12] O. Janka, S. M. Kauzlarich, *Encycl. Inorg. Bioinorg. Chem.* **2004**, pp. 1–14.
[13] H. Schäfer, B. Eisenmann, W. Müller, *Angew. Chem. Int. Ed.* **1973**, *9*, 694–712.
[14] S. Gärtner, N. Korber, *Comprehensive Inorganic Chemistry II Second Ed. From Elements to Applications* **2013**, *1*, pp. 251–267.
[15] J. D. Corbett, *Chem. Rev.* **1985**, *85*, 383–397.
[16] W. Klemm, E. Busmann, *Z. Anorg. Allg. Chem.* **1963**, *319*, 297–311.
[17] E. Zintl, *Angew. Chem.* **1939**, *52*, 1–48.
[18] E. Zintl, G. Brauer, *Z. Phys. Chem.* **1933**.
[19] R. Nesper, *Z. Anorg. Allg. Chem.* **2014**, *640*, 2639–2648.
[20] E. Hohmann, *Z. Anorg. Allg. Chem.* **1948**, *257*, 113–126.
[21] E. Busmann, *Z. Anorg. Allg. Chem.* **1961**, *313*, 90–106.
[22] T. Goebel, A. Ormeci, O. Pecher, F. Haarmann, *Z. Anorg. Allg. Chem.* **2012**, *638*, 1437–1445.
[23] L. M. Scherf, O. Pecher, K. J. Griffith, F. Haarmann, C. P. Grey, T. F. Fässler, *Eur. J. Inorg. Chem.* **2016**, *2016*, 4674–4682.
[24] C. Liu, Z. M. Sun, *Coord. Chem. Rev.* **2019**, *382*, 32–56.
[25] J. Witte, H. G. von Schnering, *Z. Anorg. Allg. Chem.* **1964**, *327*, 260–273.
[26] H. G. von Schnering, M. Schwarz, R. Nesper, *Angew. Chem. Int. Ed.* **1985**, *75*, 7360.
[27] H. G. Von Schnering, J. Llanos, Y. Grin, W. Carrillo-Cabrera, R. Nesper, *Z. Kristallogr. New Cryst. Struct.* **1998**, *213*, 662.
[28] M. Baitinger, K. Peters, M. Somer, W. Carrillo-Cabrera, Y. Grin, R. Kniep, H. G. von Schnering, *Z. Kristallogr. New Cryst. Struct.* **1999**, *214*, 455–456.
[29] C. Hoch, M. Wendorff, C. Röhr, *J. Alloys Compd.* **2003**, *361*, 206–221.
[30] H. G. von Schnering, M. Schwarz, J.-H. Chang, K. Peters, R. Nesper, *Z. Kristallogr.* **2005**, *217*, 525–527.
[31] T. Goebel, Y. Prots, F. Haarmann, *Z. Kristallogr. New Cryst. Struct.* **2008**, *223*, 187–188.
[32] T. Goebel, Y. Prots, A. Ormeci, O. Pecher, F. Haarmann, *Z. Anorg. Allg. Chem.* **2011**, *637*, 1982–1991.
[33] L. M. Scherf, M. Zeilinger, T. F. Fässler, *Inorg. Chem.* **2014**, *53*, 2096–2101.
[34] J. D. Corbett, *Angew. Chem.* **2000**, *112*, 682–704.
[35] R. Thümmel, W. Klemm, *Z. Anorg. Allg. Chem.* **1970**, *376*, 44–63.
[36] J. D. Corbett, *Inorg. Chem.* **2000**, *39*, 5178–5191.
[37] P. Pyykko, J. P. Desclaux, *Acc. Chem. Res.* **1979**, *12*, 276–281.
[38] D. A. Hansen, J. F. Smith, *Acta Crystallogr.* **1967**, *22*, 836–845.
[39] Z. C. Dong, J. D. Corbett, *J. Am. Chem. Soc.* **1994**, *116*, 3429–3435.
[40] Z. C. Dong, J. D. Corbett, *Inorg. Chem.* **1996**, *35*, 2301–2306.
[41] Z. C. Dong, J. D. Corbett, *Angew. Chem. Int. Ed.* **1996**, *35*, 1006–1009.
[42] S. Kaskel, J. D. Corbett, *Inorg. Chem.* **2000**, *39*, 778–782.
[43] D. P. Huang, Z. C. Dong, J. D. Corbett, *Inorg. Chem.* **1998**, *37*, 5881–5886.
[44] S. Gärtner, S. Tiefenthaler, N. Korber, S. Stempfhuber, B. Hischa, *Crystals* **2018**, *8*, 1–10.
[45] Z. C. Dong, J. D. Corbett, *J. Cluster Sci.* **1995**, *6*, 187–201.
[46] C. Belin, M. Tillard-Charbonnel, *Prog. Solid State Chem.* **1993**, *22*, 59–109.

[47] W. Carrillo-Cabrera, *Z. Kristallogr.* **2011**, *226*, 619–626.
[48] A. Mindraux, P. E. Bataillon, M. Cedex, *Acta Crystallogr.* **1982**, *39*, 1101–1104.
[49] W. Müller, J. Stör, *Z. Naturforsch.* **1977**, *32b*, 631–636.
[50] W. Carrillo-Cabrera, N. Caroca-Canales, H. G. von Schnering, *Z. Anorg. Allg. Chem.* **1994**, *620*.
[51] S. P. Yatsenko, K. A. Tschuntonow, A. N. Orlow, Y. P. Yarmolyuk, Y. N. Hryn, *J. Less-Common Met.* **1985**, *108*, 339–343.
[52] S. C. Sevov, J. D. Corbett, *Inorg. Chem.* **1993**, *32*, 1612–1615.
[53] J. D. Corbett, B. Li, *Inorg. Chem.* **2003**, *42*, 8768–8772.
[54] C. Slavi Sevov, J. D. Corbett, *Z. Anorg. Allg. Chem.* **1993**, *619*, 128–132.
[55] S. C. Sevov, J. D. Corbett, *J. Solid State Chem.* **1993**, *103*, 114–130.
[56] G. Cordier, V. Müller, *Z. Kristallogr.* **1993**, *203*, 150–151.
[57] B. Li, J. D. Corbett, *Inorg. Chem.* **2002**, *41*, 3944–3949.
[58] W. Carrillo-Cabrera, N. Caroca-Canales, K. Peters, H. G. von Schnering, *Z. Anorg. Allg. Chem.* **1993**, *619*, 1556–1563.
[59] V. Saltykov, J. Nuss, M. Jansen, *Z. Anorg. Allg. Chem.* **2010**, *637*, 1163–1168.
[60] V. Saltykov, J. Nuss, U. Wedig, D. L. V. K. Prasad, M. Jansen, *Z. Anorg. Allg. Chem.* **2011**, *637*, 834–839.
[61] M. Wendorff, C. Röhr, *Z. Anorg. Allg. Chem.* **2006**, *632*, 1792–1798.
[62] U. Weding, V. Saltykov, J. Nuss, M. Jansen, *J. Am. Chem. Soc.* **2010**, *132*, 12458–12463.
[63] A. Schlechte, Y. Prots, R. Niewa, *Z. Kristallogr. New Cryst. Struct.* **2004**, *219*, 381–382.
[64] H. Yamane, S. Sasaki, T. Kajiwara, T. Yamada, M. Shimada, *Acta Crystallogr. Sect. E* **2004**, *E60*, i120–i123.
[65] R. Zaremba, U. C. Rodewald, R. D. Hoffmann, R. Pöttgen, *Monatsh. Chem.* **2008**, *139*, 481–487.
[66] R. Pöttgen, *Handb. Phys. Chem. Rare Earths* **2020**, *58*, 1–38.
[67] N. L. Gulay, M. K. Reimann, Y. M. Kalychak, R. Pöttgen, *Z. Naturforsch.* **2022**, *77*, 347–352.
[68] M. Kirchner, W. Schnelle, F. R. Wagner, R. Kniep, R. Niewa, *Z. Anorg. Allg. Chem.* **2005**, *631*, 1477–1486.
[69] S. C. Sevov, J. D. Corbett, *J. Solid State Chem.* **1993**, *103*.
[70] Z. C. Dong, J. D. Corbett, *Inorg. Chem.* **1996**, *35*, 3107–3112.
[71] E. Zintl, J. Goubean, W. Dullenkopf, *Z. Phys. Chem.* **1931**, *154 A*, 1–46.
[72] E. Zintl, W. Dullenkopf, *Z. Phys. Chem. Abt. B* **1931**, 195–205.
[73] R. B. King, in *Zintl Ions* (Ed.: T. F. Fässler), King, R. B., Heidelberg, **2011**, pp. 1–24.
[74] S. Gärtner, *Crystals* **2020**, *10*, 1–26.
[75] V. F. Schwinghammer, M. Janesch, N. Korber, S. Gärtner, *Z. Anorg. Allg. Chem.* **2022**, *648*, DOI 10.1002/zaac.202200332.
[76] C. Capillas, J. M. Perez-Mato, M. I. Aroyo, *J. Phys. Condens. Matter* **2007**, *19*, 275203.
[77] D. Orobengoa, C. Capillas, M. Aroyo, J. M. Perez-Mato, *J. Appl. Crystallogr.* **2009**, *19*, 820–833.
[78] G. de la Flor, D. Orobengoa, E. Tasci, J. M. Perez-Mato, M. I. Aroyo, *J. Appl. Crystallogr.* **2016**, *49*, 653–664.
[79] G. Bergerhoff, M. Berndt, K. Brandenburg, T. Degen, *Acta Crystallogr. Sect. B* **1999**, *55*, 147–156.
[80] M. Weil, M. Shirkhanlou, *Z. Anorg. Allg. Chem.* **2017**, *643*, 757–765.
[81] D. Reichartzeder, M. Wildner, M. Weil, S. Ivanov, A. Stash, Y. S. Chen, *Eur. J. Inorg. Chem.* **2018**, *2018*, 4221–4233.
[82] A. Alkhateeb, H. Ben Yahia, *ACS Omega* **2020**, *5*, 30799–30807.
[83] B. Li, J. D. Corbett, *J. Cluster Sci.* **2008**, *19*, 331–340.
[84] L. M. Schoop, F. Pielnhofer, B. V. Lotsch, *Chem. Mater.* **2018**, *30*, 3155–3176.
[85] K. Seifert-Lorenz, J. Hafner, *Phys. Rev. B* **1999**, *59*, 829.
[86] A. Kjekshus, *Acta Chem. Scand.* **1964**, *18*, 2379–2384.
[87] C. Lorenz, S. Gärtner, N. Korber, *Crystals* **2018**, *8*, 1–17.
[88] K. Wlesler, K. Brandl, A. Fleischmann, N. Korber, *Z. Anorg. Allg. Chem.* **2009**, *635*, 508–512.
[89] C. B. Benda, T. F. Fässler, *Z. Anorg. Allg. Chem.* **2014**, *640*, 40–45.
[90] M. E. Desat, R. Kretschmer, *Chem. Eur. J.* **2018**, *24*, 12397–12404.
[91] M. E. Desat, S. Gärtner, R. Kretschmer, *Chem. Commun.* **2017**, *53*, 1510–1513.
[92] C. Lorenz, F. Hastreiter, J. Hioe, N. Lokesh, S. Gärtner, N. Korber, R. M. Gschwind, *Angew. Chem. Int. Ed.* **2018**, *57*, 12956–12960.
[93] T. Henneberger, W. Klein, T. F. Fässler, *Z. Anorg. Allg. Chem.* **2018**, *644*, 1018–1027.
[94] F. Hastreiter, C. Lorenz, J. Hioe, S. Gärtner, N. Lokesh, N. Korber, R. M. Gschwind, *Angew. Chem. Int. Ed.* **2019**, *58*, 3133–3137.
[95] C. C. Yu, A. Ormeci, I. Veremchuk, X. J. Feng, Y. Prots, M. Krnel, P. Koželj, M. Schmidt, U. Burkhardt, B. Böhme, L. Akselrud, M. Baitinger, Y. Grin, *Inorg. Chem.* **2023**, DOI 10.1021/acs.inorgchem.3c00790.
[96] CrysAlisPro, Version 41_64.93a, Oxford Diffraction/Agilent Technologies UK Ltd. Yarnton, UK **2020**.
[97] G. M. Sheldrick, *Acta Crystallogr. Sect. A* **2015**, *71*, 3–8.
[98] G. M. Sheldrick, *Acta Crystallogr. Sect. C* **2015**, *71*, 3–8.
[99] V. Petricek, M. Dusek, L. Palatinus, *Z. Kristallogr.* **2014**, *299*, 345–352.
[100] K. Eichele, *WSolids1. vers. 1.20.20* **2013**, Universität Tübingen.
[101] H. Eschrig, *Phys. Rev. B* **1999**, *59*, 1743–1757.
[102] H. Eschrig, K. Koepernik, I. Chaplygin, *J. Solid State Chem.* **2003**, *176*, 482–495.
[103] H. Eschrig, *Phys. Rev. B* **1999**, *60*, 14035–14041.
[104] K. Lejaeghere, G. Bihlmayer, T. Björkman, P. Blaha, S. Blügel, V. Blum, D. Caliste, I. E. Castelli, S. J. Clark, A. Dal Corso, S. De Gironcoli, T. Deutsch, J. K. Dewhurst, I. Di Marco, C. Draxl, M. Dułak, O. Eriksson, J. A. Flores-Livas, K. F. Garrity, L. Genovese, P. Giannozzi, M. Giantomassi, S. Goedecker, X. Gonze, O. Grånäs, E. K. U. Gross, A. Gulans, F. Gygi, D. R. Hamann, P. J. Hasnip, N. A. W. Holzwarth, D. Iuşan, D. B. Jochym, F. Jollet, D. Jones, G. Kresse, K. Koepernik, E. Küçükbenli, Y. O. Kvashnin, I. L. M. Locht, S. Lubeck, M. Marsman, N. Marzari, U. Nitzsche, L. Nordström, T. Ozaki, L. Paulatto, C. J. Pickard, W. Poelmans, M. I. J. Probert, K. Refson, M. Richter, G. M. Rignanese, S. Saha, M. Scheffler, M. Schlipf, K. Schwarz, S. Sharma, F. Tavazza, P. Thunström, A. Tkatchenko, M. Torrent, D. Vanderbilt, M. J. Van Setten, V. Van Speybroeck, J. M. Wills, J. R. Yates, G. X. Zhang, S. Cottenier, *Science* **2016**, *351*, DOI 10.1126/science.aad3000.
[105] F. Wang, U. Wedig, D. L. V. K. Prasad, M. Jansen, *J. Am. Chem. Soc.* **2012**, *134*, 19884–19894.
[106] J. P. Perdew, K. Burke, M. Ernzerhof, *Phys. Rev. Lett.* **1996**, *77*, 3865–3868.
[107] Origin(Pro), Version 9.9.0.225, OriginLab Corporation, Northampton, MA, USA **2021**.

Manuscript received: May 26, 2023
Revised manuscript received: July 31, 2023
Accepted manuscript online: August 8, 2023

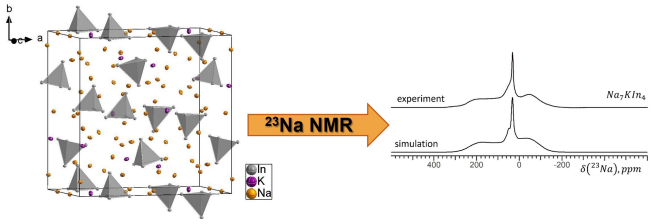

*M. Janesch, V. F. Schwinghammer, Dr. I. G. Shenderovich, Dr. S. Gärtner**

1 – 9

Synthesis and characterization of ternary trielides Na_7KTr_4 [*Tr* = In or Tl] including $[Tr_4]^{8-}$ Tetrahedra